CRITERIA FOR SKIN RUPTURE AND CORE SHEAR CRACKING DURING IMPACT ON SANDWICH PANELS

R. Olsson[1]*, TB. Block[2]
[1] Swerea SICOMP, Mölndal, Sweden, [2] Faserinstitut Bremen, University of Bremen, Germany
* Corresponding author (robin.olsson@swerea.se)

Keywords: *Impact, Core shear cracks, Sandwich panels, Foam cores*

1 Summary

Core shear cracking induced by impact on sandwich panels is a detrimental failure mode causing severe loss of structural performance. This paper derives analytical expressions for initiation of skin rupture and core shear cracking during impact on sandwich panels with foam cores. The criteria are successfully validated by comparison with experimental results for a range of thicknesses of skins and cores in panels with carbon/epoxy NCF skins and a Rohacell foam core.

2 Introduction

Sandwich panels with laminated composite skins offer very high bending stiffness per unit weight and are therefore attractive for use in aircraft structures, but concerns remain over damage tolerance issues [1]. Models have therefore been developed to predict impact response and damage [2, 3]. Most aircraft structures have used honeycomb cores, which offer high shear stiffness, but have been found to cause problems with water entrapment. This problem is avoided with foam cores, which also offer simplified manufacturing, but a major concern is the risk for core shear cracking or skin debonding, e.g. due to impact, which may reduce structural performance severely, Fig 1. [3].

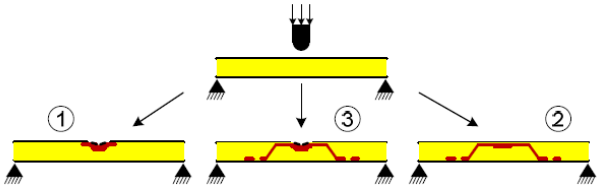

Fig. 1. Impact damage involving core crushing and (1) skin rupture, (2) core shear cracking and (3) combined skin rupture and core shear cracking [3].

The phenomenon of foam core shear cracking in sandwich panels due to impact has, however, yet received only limited attention. Previously core shear cracking has been observed after impact on large panels with GFRP skins with PVC foam cores, for use in naval applications [4]. Leijten et. al. [5] analyse the impact resistance and compressive residual strength of CFRP foam core sandwich panel with PMI foams for application in primary aircraft structures. They describe a significant increase in planar damage area during non-destructive inspection (NDI) for a particular sandwich configuration with a relatively thin foam core but otherwise concentrate on skin debonding due to core crushing below the point of impact. Destructive sectioning of this particular sandwich configuration revealed core shear cracks that emerge from the local core crushing area and extend in a circular manner conically through the foam core. These shear cracks result in a reduced flexural stiffness of the affected specimens compared to the reference configuration.

A more general review on the effects of impact on sandwich panels, and a comparison of damage types in various skin and core materials was provided by Abrate [6]. Honeycomb cores are less vulnerable to shear cracking as through the thickness crack growth has to rupture the cell walls. Shear loads on honeycomb cores instead typically lead to shear buckling of the cell walls. An extensive investigation of Nomex honeycomb core sandwich panels with CFRP face sheets by Raju et. al [7] revealed no core shear cracking as failure mode. It is however reported that with decreasing core thickness and increasing diameter of the indenter, the planar damage area in the sandwich increases, too.

3 Theory

Impact and static indentation of sandwich panels with composite laminate skins result in a sequence of damage events. The local elastic face sheet deflection is typically followed by core crushing, face sheet delamination and eventually skin rupture. Foam cores frequently also experience core shear cracking. A typical load-indentation curve for a panel without core shear cracking is shown in Fig. 2.

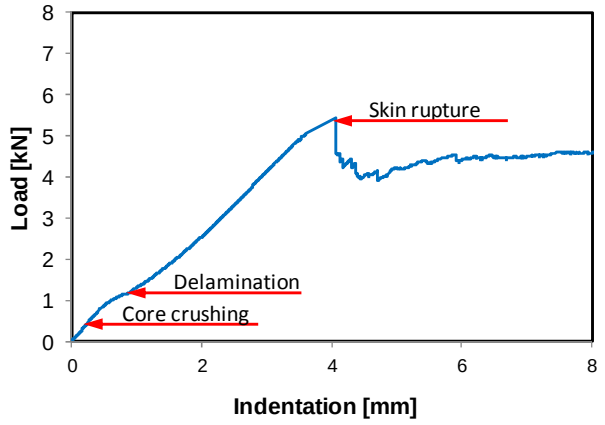

Fig. 2. Typical load-indentation curve for a sandwich panel without shear cracking.

Core crushing involves initial elastic buckling of the core cell walls, followed by cracking or plastic buckling of the cell walls. Cellular core materials have been found to crush under a more or less constant compressive stress, p_{cr}, up to the point of densification (>80% strain) where the cell walls are entirely collapsed and the core modulus approaches the modulus of the solid cell wall material [8].

The following theory is based on consideration of vertical equilibrium for a hemisphere of radius R indenting a sandwich panel with a skin of thickness h_f, and a core of thickness h_c being crushed within a radius a, as illustrated in Fig. 3.

The effective (axisymmetric) plate stiffness in bending of the skin is given by D_f^* [2]:

$$D_f^* \approx \sqrt{D_{f11} D_{f22} (\eta + 1)/2} \qquad (1)$$

$$\text{where } \eta = \left(D_{f12} + 2D_{f66}\right) \Big/ \sqrt{D_{f11} D_{f22}}$$

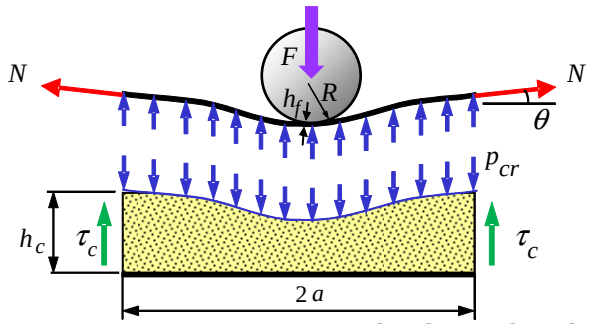

Fig. 3. Forces acting on a sandwich panel with a central crush zone of radius a.

Here $D_{f\,ij}$ are the elements of the bending stiffness matrix of the skin, as given by laminate theory. We now define effective moduli Q_f^* of the skin (subscript "f") and Q_c^* of the core (subscript "c"):

$$Q_f^* = 12 D_f^* / h_f^3 \qquad Q_c^* = \begin{cases} E_c / \left(1 - \nu_c^2\right) & \text{foam} \\ E_{cz} & \text{honeycomb} \end{cases} \qquad (2)$$

where "z" refers to the thickness direction [2]. The elastic face sheet deflection under a concentrated load F is modelled as a plate on an elastic foundation, where the foundation stiffness is influenced by the stiffness and thickness of the face sheet and core. The core may be considered semi-infinite when the core thickness h_c exceeds a certain maximum value h_{cmax} [2]:

$$h_{c\max} = h_f \tfrac{32}{27} \left(\tfrac{4}{3} Q_f^* / Q_{cz}^*\right)^{1/3} \qquad (3)$$

The load for onset of core crushing, F_{cr}, is given by the theory for centrally loaded plates on an elastic foundation, and has been derived previously [2]:

$$F_{cr} = 4 p_{cr} \sqrt{Q_f^* h_f^3 h_c / \left(4.14 Q_{cz}^*\right)} \qquad \text{for } h_c \le h_{c\max} \qquad (4)$$

$$F_{cr} = 3\sqrt{3}\, p_{cr} \left[Q_f^* h_f^3 / \left(6 Q_{cz}^*\right)\right]^{2/3} \qquad \text{for } h_c > h_{c\max}$$

which have been rewritten using the first relation in Eq. (2). The load for onset of skin delamination, F_{d1}, has been derived previously [2], and may be written:

$$F_{d1} = \pi \sqrt{8 Q_f^* h^3 G_{IIc} / 9} \qquad (5)$$

where G_{IIc} is the interlaminar toughness in mode II. The delamination threshold load is the same as for

monolithic laminates, since the core support is negligible for an infinitesimally small delamination, but increases somewhat for subsequent delamination growth, due to increasing core support.

Skin delamination occurs at an early stage and causes a more or less complete loss of skin bending stiffness, while membrane action is maintained. Hence skin rupture may be predicted by considering the equilibrium of a membrane wrapped around a hemispherical impactor. In the contact region the delaminated skin obtains the shape of a spherical cap, with a resulting uniform contact pressure, Fig. 4.

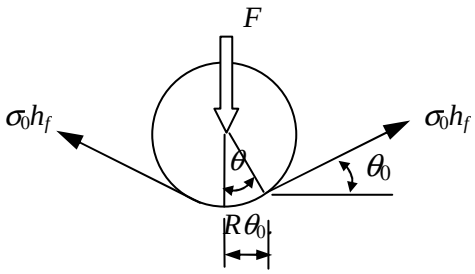

Fig. 4. Geometry of a membrane wrapping around a hemispherical impactor/indentor.

Thus, the membrane is in a state of uniform plane stress, where the stress-strain relation is given by:

$$\sigma_0 = \varepsilon_0 E_r^* / \left(1-\nu_r^*\right) \qquad (6)$$

where E_r* and ν_r* are the average Young's modulus and Poisson's ratio of the skin. These properties are obtained by evaluating the average values of a ply rotated a complete circle, and are identical to the corresponding properties for a quasi-isotropic laminate. The membrane strain at the edge of the contact area is given by the relation between membrane strains and slope:

$$\varepsilon_0 = \theta_0^2 / 2 \qquad (7)$$

Vertical equilibrium for the spherical cap gives:

$$F = 2\pi R\theta_0 \cdot \sigma_0 h\theta_0 = 2\pi R\sigma_0 h\theta_0^2 \qquad (8)$$

Combination with Eqs (6)-(7) gives the expression:

$$F = 4\pi R h_f E_r^* \varepsilon_0^2 / \left(1-\nu_r^*\right) \qquad (9)$$

The resulting skin rupture load F_r is obtained by evaluating the load for a strain ε_0 equal to the ultimate tensile failure strain ε_{1t}:

$$F_r = 4\pi R h_f E_r^* \varepsilon_{1t}^2 / \left(1-\nu_r^*\right) \qquad (10)$$

Impact and indentation of sandwich panels typically results in a central zone with core crushing. The radius a of the crush zone is obtained from equilibrium between the contact load F, the core crush reaction and the skin membrane load N at the edge of the crush zone, Fig. 3:

$$p_{cr}\pi a^2 = F - 2\pi a N\theta \qquad (11)$$

The squared radius may be written on the following dimensionless form:

$$\bar{a}^2 = p_{cr}\pi a^2 / F = 1 - 2\pi a N\theta / F \qquad (12)$$

where $2\pi aN\theta/F$ is a reduction factor accounting for the load carried by skin membrane action during indentation. Solutions for the indentation of a sandwich skin on a crushing core, and relations between a and F were presented in [9].

Classical sandwich plate theory assumes a uniform shear stress over the core thickness. The core shear stress increases proportionally to the radius in the region with constant crush stress, and decreases outside this region due to decreasing contact stresses between skin and core. Hence, from Fig. 3 the peak core stress τ_c is given by the following relation:

$$\tau_c = \frac{p_{cr}\pi a^2}{2\pi a h_c} = \frac{p_{cr} a}{2h_c} = \frac{1}{h_c}\sqrt{\frac{F\bar{a}^2 p_{cr}}{4\pi}} \qquad (13)$$

where the relations in Eq. (12) have been used. The load is limited by the skin rupture load F_r. Hence the maximum shear stress $\tau_{c\max}$ in the core is given by:

$$\tau_{c\max} = \sqrt{F_r \bar{a}_r^2 p_{cr} / (4\pi)} / h_c \qquad (14)$$

$$= \sqrt{R h_f E_r^* \bar{a}_r^2 p_{cr} / \left(1-\nu_r^*\right)} \cdot \varepsilon_{1t} / h_c$$

where $\bar{a}_r$ is the dimensionless crush radius at the rupture load F_r. The results in [9] show that $\bar{a}^2 \leq 0.8$, and hence a value $\bar{a}_r^2 \approx 0.8$ may be used for conservative design.

4 Experiments

Sandwich panels were made from 75 kg/m^3 Rohacell PMI RIST foam cores covered with skins of HTS carbon non-crimp fabric (NCF) impregnated by RTM6 epoxy resin. The face sheets have a stacking sequence of $[(45/0/\text{-}45)_s]_n$ and a ply thickness of 0.125 mm leading to total laminate thicknesses of 0.75 mm, 1.5 mm, 2.25 mm and 3.0 mm. The core thickness varies between 6.5 mm and 35.5 mm. The complete test matrix with all configurations is shown in Table 1. For each sandwich configuration three specimens were manufactured and tested with variable impact energies.

Tab. 1. Test matrix of impact tests.

Skin thickness h_f [mm]	Core thickness, h_c [mm]				
	6.5	10.0	16.3	25.7	35.5
0.75	x	x	x		
1.50	x	x	x	x	x
2.25			x	x	x
3.00			x	x	x

Impact tests were performed by the Fraunhofer Institute for Mechanics of Materials in Halle, Germany. A drop weight impact testing machine was used with a 3.1 kg impactor and a hemispherical tup of radius R=12.7 mm. This impactor is considered more critical compared to smaller types, as it increases the loading on the weaker core material due to shear bending.

For the impact tests the sandwich panels were cut to a size of 350 x 400 mm and fixed inside a rigid picture frame with a 250 x 300 mm window as shown in Figure 5. Impacts were applied to the centre of the specimen with impact energies varying from 12 J to 90 J depending on the strength of the specimen. The size of the test specimens was selected large in order to reduce edge effects and keep the thickness of the test specimens by one order of magnitude smaller than its in-plane dimensions representative for shell structures.

Impactor load and displacement were recorded during the experiments and skin and core damage inspected afterwards using air-coupled ultrasonics, and in some cases also fractography of sections cut from panels. The load and displacement curves thus characterize the impact process itself while the damage measurements characterize the damaged specimen.

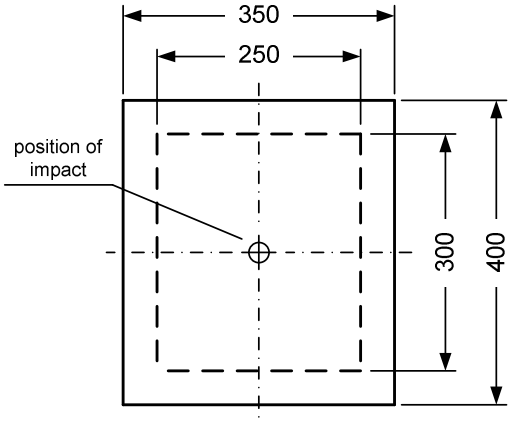

Fig. 5. Sandwich plates and picture frame used for specimen fixture during impact testing.

Figure 6 displays the peak impact load observed during testing. The results are grouped by two categories. The shape of the symbol is selected depending on the skin thickness. Filled symbols mark specimens with observed core shear cracking while empty symbols represent specimens where there was only local core damage occurring.

It can be observed that the peak impact force is constant for all specimens of the same face sheet thickness and impact energies above a certain threshold energy. From investigation of damaged specimens this threshold energy can be related to face sheet rupture which coincides with the peak force observed during impact testing. Consequently core shear cracking as a damage mode has – if at all – only little influence.

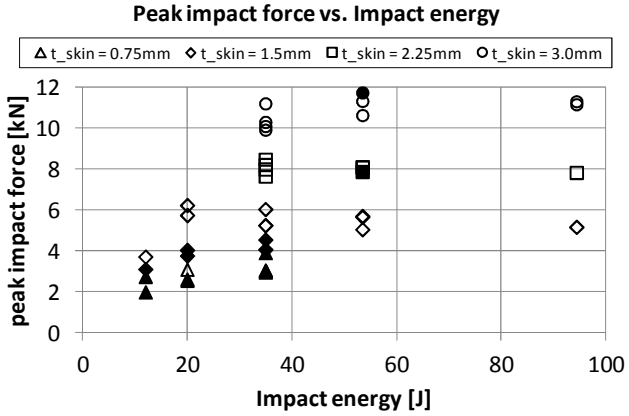

Fig. 6. Peak impact force vs. impact energy. Filled symbol = observed core shear cracking, Empty symbol = local core damage.

Figure 7 shows the planar damage diameter observed in the damaged test specimens. The results show only total damage area and do not distinguish between face sheet and core damage. Core damage was observed either in the form of local face sheet debonding due to core crushing below the point of impact or in the form of additional core shear cracking. In any case core damage was observed larger than face sheet damage and thus describes the total damage area fully.

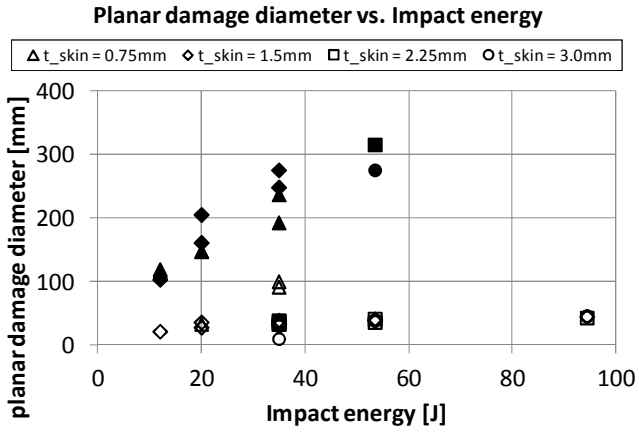

Fig. 7. Planar damage diameter vs. impact energy. Filled symbol = observed core shear cracking, Empty symbol = local core damage.

When looking at the graph two trends become obvious as the results arrange depending on the observed damage mode. Specimens with core shear cracking (filled symbols) are subject to significantly larger damage sizes at lower impact energies than specimens with a local core damage observed. Here a maximum damage size of 50 mm diameter was observed compared to a maximum damage size of about 300 mm for specimens with core shear cracking, which is close to the total size of the specimen.

Only one particular specimen did not fit into either of the two trends. The specimen has a very thin face sheet of only 0.75 mm, a 16.3 mm thick core and was impacted with a relatively high energy of 35 J. The measured damage diameter was 100 mm and was confirmed by sectioning. This also revealed that the impactor had punctured the front face sheet and crushed almost through the entire core. As the impactor approached the rear face sheet, it created a local debonding of the rear face sheet which was captured by the NDI and thus explains the large damage size. The damage mode however is core crushing combined with face sheet rupture.

Destructive sectioning was also performed on selected specimens in order to confirm the available NDI results. Fig. 8 shows the damage mode local core crushing with skin rupture while Fig. 9 shows foam core shear cracking. Both specimens shown have a 2.25 mm thick face sheet and where subject to a 50 J impact. The core thickness differs however as the specimen in Fig. 8 has got a 35.5 mm thick core while the foam core of the specimen in Fig. 9 is only 16.3 mm thick.

Fig. 8. 50 J impact damage in a specimen with a ‘thick’ core: Core crushing with face sheet rupture.

Fig. 9. 50 J impact damage in a specimen with a 'thin' core: Core crushing extended by a foam core shear crack.

5 Comparison between theory and experiments

Theoretical predictions were based on the following elastic properties for the individual UD-plies of the NCF material: E_1=130 GPa, E_2=9 GPa, G_{12}=4.5 GPa and ν_{12}=0.26. The value of E_1 reported in [3] has been slightly reduced to better reflect the stiffness reduction caused by fibre crimp in NCF composites. The resulting average (quasi-isotropic) skin properties are: E_r^*=50 GPa, ν_r^*=0.307. The tensile failure strain was assumed to be ε_{1t}=1.8 %, based on the failure strain for fibre bundles reported by the fibre manufacturer [10]. This value is significantly higher than the tensile failure strain for conventional coupons of the NCF bulk material, but is thought to be more representative of the small material volumes (a few mm^3) strained under the impactor. The increasing strength for small material volumes is a well known result of Weibull's statistical theory of strength [11].

The following properties were assumed for the 75 kg/m^3 RIST foam: p_{cr}=1.7 MPa, τ_U=1.3 MPa [12]. Furthermore the dimensionless squared crush radius was assumed to be $\bar{a}_r^2 = 0.8$ [2].

Figure 10 gives a comparison between predicted and experimentally observed load for onset of skin rupture, which coincides with the peak load during impact. To illustrate the effect of skin failure strain, predictions for a failure strain of 1.6 % (obtained in conventional tests on bulk material) and 2.0 % have been included for comparison.

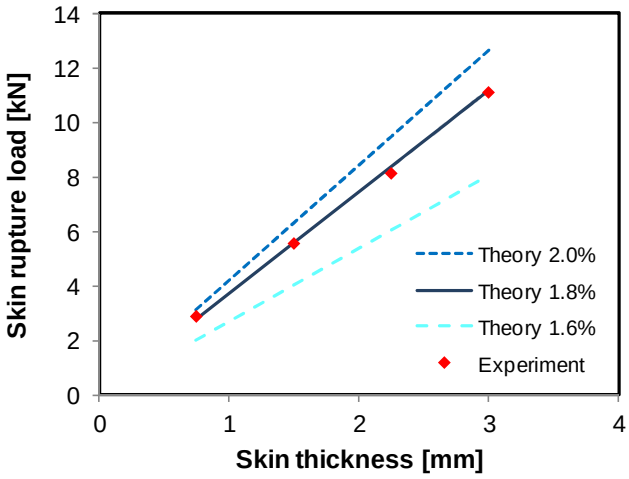

Fig. 10. Comparison between predicted skin rupture load and experimentally observed peak load.

Figure 11 presents curves for predicted shear stress, and symbols representing corresponding experimental observations of core shear cracking. It is evident that the appearance of shear cracks closely corresponds to predicted stresses exceeding the shear strength of the foam core material and that core shear cracking can be prevented by exceeding a certain critical core thickness.

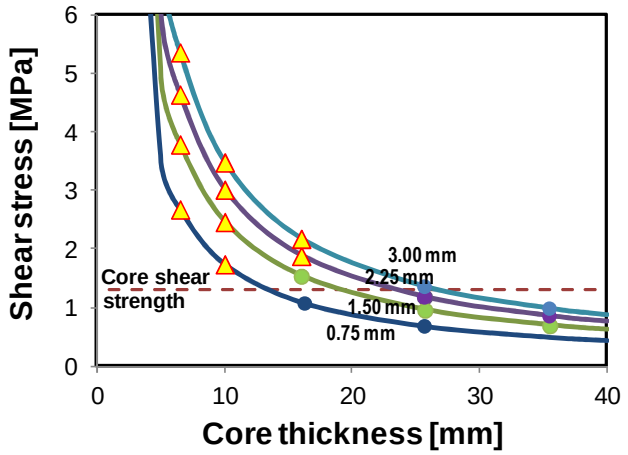

Fig. 11. Predicted core shear stress and observed core shear cracking. Triangle=observed core cracking, Circle= no observed shear cracking.

6 Discussion and conclusions

Impact resistance is an important part of damage tolerance which is required for primary load bearing structures in aircraft. Here impact resistance is the ability of a structure to withstand impact loads with minimum damage. In contrast to this damage tolerance is the ability of a structure to sustain maximum load bearing capability without catastrophic failure despite undetected structural damage. As impact events are a common source of damage, increasing the impact resistance of a structure may reduce the required damage tolerance performance.

For monolithic CFRP structures impact resistance is typically determined by measuring damage caused by relevant impact threats. This is then correlated with the appropriate NDI technique - typically visual inspection - in order to confirm whether the damage is detectable or not. From this correlation the maximum damage, that is not detectable, has to be used for damage tolerance analysis and tested experimentally by e.g. compression after impact.

The impact resistance of CFRP sandwich structures is typically determined the same way. During impact tests with various sandwich configurations two types of damage modes in foam core sandwich structures have been observed. The first damage mode – core crushing combined with face sheet rupture – creates limited damage sizes in the core and typically has got a good visibility. The second damage mode – core crushing extended by core shear cracks – creates significantly larger damage sizes and typically has got less visibility.

From a damage tolerance point of view core crushing and face sheet rupture can be treated similar to monolithic CFRP. Core shear cracking however is more detrimental to the damage tolerance performance as it creates larger damage sizes at less visibility. Avoidance of foam core shear cracking could thus lead to significant improvement of the damage tolerance of sandwich structures.

In this work criteria for skin rupture (penetration) and core shear cracking of CFRP foam core sandwich panels during low velocity blunt impact have been presented and compared with experimental results. Good agreement between experiments and the damage criteria has been reached.

By applying these criteria e.g. during preliminary design, the damage mode of sandwich structures subject to a relevant impact threat can be estimated and e.g. by design changes altered in order to improve the damage tolerance performance. It is noted that prevention of skin rupture and core shear cracking may be partly conflicting aims. Skin rupture is prevented by increasing the stiffness (modulus and/or thickness) or tensile failure strain of the skin. These modifications are however detrimental for core shear cracking.

Core shear cracking is prevented by reducing the core shear failure index τ_{cmax}/τ_U, where τ_U is the shear strength of the core. Inspection of Eq. (14) reveals that this may be done in several ways. Reduction of the skin failure strain or modulus is rarely an option as this reduces the mechanical performance of the panel. Core modification involves increasing the density or thickness of the core. Both have a similar weight penalty, but it is evident that an increased core thickness is more weight efficient, as the crush stress p_{cr} and shear strength τ_U of foams both are approximately proportional to the core density.

It has to be kept in mind however that the presented failure criteria are limited to simple geometries and load cases and do not account for material non-linearity such as e.g. strain rates, plasticity of the foam core or residual stresses dating back to manufacturing of the sandwich structure.

Acknowledgements

The authors thank the CTC Stade GmbH for manufacturing of the test specimens as well as Martin Rinker and Marianne John of the Fraunhofer Institute for Mechanics of Materials in Halle, Germany for impact testing of the specimens.

References

[1] Zuardy MI, Herrmann AS. An advanced centre box of a vertical tail plane with a side panel from CFRP foam-core sandwich structure. *CEAS Aeronaut J* 2011;2(1-4):253-269.

[2] Olsson R. Engineering method for prediction of impact response and damage in sandwich panels. *J Sandwich Struct Mater* 2002;4(1):83-95.

[3] Block TB, Brauner C, Zuardy MI, Herrmann AS. Advanced numerical investigation of the impact behaviour of CFRP foam core sandwich structures. Proc 3rd ECCOMAS Thematic Conf on the Mechanical Response of Composites. Hannover, Germany, 21-23 September 2011.

[4] Wiese M, Echtermeyer A, Hayman B. Evaluation of oblique impact damage on sandwich panels with PVC and balsa core materials. Proc Fourth Int Conf on Sandwich Construction. Stockholm, Sweden, 9-11 June 1998. EMAS Publ:807-818.

[5] Leijten J, Bersee HEN, Bergsma OK, Beukers A. Experimental study of the low-velocity impact behaviour of primary sandwich structures in aircraft. *Composites: Part A* 2009; 40: 164-175.

[6] Abrate S. Localized impact on sandwich structures with laminated facings. *Applied Mechanics Reviews*. 1997;50(2):69-82.

[7] Raju KS, Smith BL, Tomblin JS, Liew KH, Guarddon JC. Impact damage resistance and tolerance of honeycomb core sandwich panels. *J Composite Materials* 2008;42(4):385-412.

[8] Gibson LJ, Ashby MF. *Cellular solids*. 2nd ed. Cambridge University Press. Cambridge 1999.

[9] Olsson R, McManus HL. Improved theory for contact indentation of sandwich panels. *AIAA J*. 1996;34(6):1238-1244.

[10] HTS 5631 800/1600tex 12/24K t0/Z10 data sheet. *Document PLS 017 Rev E 01/29/07*. Toho Tenax America Inc, 2007.

[11] O'Brien TK, Salpekar SA. Scale effects on the transverse tensile strength of graphite epoxy composites. In: Composite materials and design (Eleventh volume), *ASTM STP1206*, Ed: Camponeschi ET, Jr. ASTM, Philadelphia 1993:23-52 (also NASA TM 107637).

[12] *Product information: ROHACELL RIST*. January 2011 edition. Evonik Industries. Darmstadt, Germany.